The Plant Cell, Vol. 20: 3331–3345, December 2008, www.plantcell.org

Characterization of *Raphanus sativus* Pentatricopeptide Repeat Proteins Encoded by the Fertility Restorer Locus for Ogura Cytoplasmic Male Sterility [W]

M. Uyttewaal,[a,b] N. Arnal,[a] M. Quadrado,[a] A. Martin-Canadell,[a] N. Vrielynck,[a] S. Hiard,[a] H. Gherbi,[c,1] A. Bendahmane,[c] F. Budar,[a] and H. Mireau[a,2]

[a] Institut National de la Recherche Agronomique, Station de Génétique et d'Amélioration des Plantes, 78026 Versailles, France
[b] Ecole Normale Supérieure, Laboratoire de Reproduction et Développement des Plantes, 69364 Lyon, France
[c] Institut National de la Recherche Agronomique, Unité de Recherches en Génomique Végétale, 91057 Evry, France

Cytoplasmic male sterility is a maternally inherited trait in higher plants that prevents the production of functional pollen. Ogura cytoplasmic male sterility in radish (*Raphanus sativus*) is regulated by the *orf138* mitochondrial locus. Male fertility can be restored when *orf138* accumulation is suppressed by the nuclear *Rfo* locus, which consists of three genes putatively encoding highly similar pentatricopeptide repeat proteins (PPR-A, -B, and -C). We produced transgenic rapeseed (*Brassica napus*) plants separately expressing *PPR-A* and *PPR-B* and demonstrated that both encoded proteins accumulated preferentially in the anthers of young flower buds. Immunodetection of ORF138 showed that, unlike PPR-B, PPR-A had no effect on the synthesis of the sterility protein. Moreover, immunolocalization experiments indicated that complete elimination of ORF138 from the tapetum of anthers correlated with the restoration of fertility. Thus, the primary role of PPR-B in restoring fertility is to inhibit ORF138 synthesis in the tapetum of young anthers. In situ hybridization experiments confirmed, at the cellular level, that PPR-B has no effect on the accumulation of *orf138* mRNA. Lastly, immunoprecipitation experiments demonstrated that PPR-B, but not PPR-A, is associated with the *orf138* RNA in vivo, linking restoration activity with the ability to directly or indirectly interact with the *orf138* RNA. Together, our data support a role for PPR-B in the translational regulation of *orf138* mRNA.

INTRODUCTION

Cytoplasmic male sterility (CMS) is a widespread phenomenon in plants and represents a condition in which plants fail to produce functional pollen (Chase, 2007). It is a maternally inherited trait generally governed by unusual and often chimeric mitochondrial open reading frames (Hanson and Bentolila, 2004). In many instances, male sterility can be reverted to male fertility through the action of one or several nuclear loci, called fertility restorer (*Rf*) genes. Allelic copies (*rf*) of restorer genes that do not restore male fertility are denoted as maintainers of fertility. In addition to being exploited for hybrid production, CMS/*Rf* systems represent molecular models for studying the genetic relationship and functional cooperation between mitochondrial and nuclear genomes in plants (Chase, 2007). The Ogura CMS, originally identified in radish (*Raphanus sativus*) and later transferred to rapeseed (*Brassica napus*), is controlled by the mitochondrial *orf138* locus that consists of two cotranscribed open reading frames, *orf138* and *orfB* (or *atp8*, encoding ATP synthase subunit 8) (Bonhomme et al., 1991, 1992). In contrast with many sterility-inducing proteins, ORF138 is not a chimeric polypeptide composed of fragments of conventional mitochondrial proteins. The ORF138 protein was recently shown to reside in the inner membrane of mitochondria, likely assembled as a homopolymer, but the mechanism by which it interferes with pollen production is still unclear (Grelon et al., 1994; Duroc et al., 2005). Nevertheless, because the expression of *orf138* was shown to strongly inhibit bacterial growth, ORF138 is presumed to produce a certain level of toxicity toward mitochondrial activity in the tapetum of anthers (Duroc et al., 2005). Several groups recently succeeded in cloning the Ogura CMS restorer locus, *Rfo*, in radish by positional cloning (Brown et al., 2003; Desloire et al., 2003; Koizuka et al., 2003). The *Rfo* locus contains three genes organized in tandem, arbitrarily named *PPR-A*, *PPR-B*, and *PPR-C*, which are predicted to encode highly similar proteins. *PPR-B* was genetically defined as the restorer gene and is predicted to encode a pentatricopeptide repeat (PPR) protein belonging to the P subfamily of PPR genes and comprising 17 PPR repeats (Lurin et al., 2004). The predicted PPR-A protein possesses a longer C-terminal tail and a deletion of four amino acids in the third PPR repeat, compared with PPR-B; overall, the two proteins are 87% identical at the amino acid level. The coding capacity of *PPR-C* is less clear, as the gene contains a 17-bp deletion compared with *PPR-A* and *PPR-B*, which leads to a frameshift and a premature stop codon in roughly the middle of

[1] Current address: IRD-911, Avenue Agropolis, BP 64501, 34394 Montpellier, France.
[2] Address correspondence to mireau@versailles.inra.fr.
The author responsible for distribution of materials integral to the findings presented in this article in accordance with the policy described in the Instructions for Authors (www.plantcell.org) is: H. Mireau (mireau@versailles.inra.fr).
[W] Online version contains Web-only data.
www.plantcell.org/cgi/doi/10.1105/tpc.107.057208

the gene. It was suggested that this frameshift could be corrected by splicing a predicted intron, creating a 30–amino acid deletion in PPR repeats 6 and 7 (Desloire et al., 2003). The genetic organization of the *Rfo* locus is not unique; restorer genes are often found in clusters of PPR genes or surrounded by highly related PPR genes. The restoration locus in petunia (*Petunia hybrida*) bears two tandemly arranged and highly homologous PPR genes encoding proteins that are 93% similar (Bentolila et al., 2002). The rice (*Oryza sativa*) *Rf-1* locus also carries several PPR genes, among which two encode proteins of different sizes, but with 70% identity, and both can restore fertility (Wang et al., 2006). Thus, grouping of similar PPR genes at distinct loci appears to be a characteristic of *Rf* and *Rf*-like PPR genes and may be a consequence of an active evolutionary expansion, possibly governed by diversifying selection, as proposed by Geddy and Brown (2007).

PPR proteins are characterized by tandem arrays of degenerate 35–amino acid motifs (Small and Peeters, 2000). This protein family is extraordinarily large in higher plants and contains 450 members in *Arabidopsis thaliana*, 477 in rice, and 103 in the moss *Physcomitrella patens* (O'Toole et al., 2008). The majority of these proteins are predicted to target chloroplasts or mitochondria (Lurin et al., 2004). By analogy to tetratricopeptide repeats, PPR modules are thought to form specific interaction domains, and coimmunoprecipitation or other in vitro assays showed that several PPR proteins associate with RNA (Lahmy et al., 2000; Nakamura et al., 2003; Lurin et al., 2004; Schmitz-Linneweber et al., 2005, 2006; Gillman et al., 2007; Beick et al., 2008; Kazama et al., 2008; Williams-Carrier et al., 2008). Although the modes of action of these proteins are not known in any detail, PPR proteins were proposed to act by recruiting RNA-modifying activities to specific RNA target sites. In *Arabidopsis*, bioinformatics analyses distinguished two PPR protein subfamilies of equal size, based on the presence of a type of PPR repeat and also an additional C-terminal domain (Lurin et al., 2004). P-type PPR proteins are composed of classical 35–amino acid repeats, whereas PLS proteins, which are specific to land plants, exhibit tandem repeats of three PPR variant motifs. PLS proteins were further classified into four categories based on the presence or absence of C-terminal domains, termed E, E+, and DYW.

Data have strongly implicated PPR proteins in various steps of organellar gene expression, mostly in relation to RNA expression. In this context, plant PPR proteins were shown to be key factors in translation (Fisk et al., 1999; Yamazaki et al., 2004; Uyttewaal et al., 2008), intron splicing (Meierhoff et al., 2003; Schmitz-Linneweber et al., 2006; de Longevialle et al., 2007, 2008), mRNA stabilization (Yamazaki et al., 2004, Beick et al., 2008), editing (Kotera et al., 2005; Okuda et al., 2007), and RNA cleavage (Hashimoto et al., 2003; Meierhoff et al., 2003; Hattori et al., 2007). Most of these reports, however, focused on plastid PPR proteins, and very few detailed studies were performed on plant mitochondria. Besides *Rfo*, several other fertility-restorer genes were shown to encode members of the PPR family. Notably, the petunia *Rf592* gene that prevents expression of the *pcf* (for petunia CMS-associated fused) sterility gene through an undetermined mechanism (Bentolila et al., 2002) encodes a protein that associates with *pcf* RNA in vivo (Gillman et al., 2007). Two rice *Rf* genes, *Rf1a* and *Rf1b*, present within the same locus, can suppress the expression of the Boro II CMS-associated *orf79* via different mechanisms (Wang et al., 2006; Kazama et al., 2008). The RF1A protein prevents the synthesis of ORF79 by cleaving the B-*atp6*/*orf79* bicistronic RNA, a phenomenon that affects both the stability and the translational activity of *orf79* transcripts. RF1B acts by mediating the degradation of the B-*atp6*/*orf79* transcripts. The fertility restorer of the A1-type CMS in sorghum (*Sorghum bicolor*) was also shown to encode a PPR protein, but the molecular mechanism underlying restoration is unclear, as the mitochondrial gene responsible for sterility is still unknown in this system (Klein et al., 2005).

In order to further understand the molecular mechanisms governing fertility restoration in the Ogura system and to identify key functional differences between the different members of the *Rfo* cluster, we produced transgenic rapeseed plants independently expressing two of the three radish PPR genes present at the *Rfo* locus. A detailed analysis of these plants was performed, with a focus on the accumulation of the PPR-A and PPR-B proteins in reproductive tissues and on the elimination of ORF138 and its consequences on fertility restoration. We also investigated the association of PPR-A and PPR-B with *orf138* mRNA, and our findings indicated that fertility restoration is correlated with an in vivo association between PPR-B and the mRNA of the sterility gene.

RESULTS

Production of Rapeseed Transgenic Plants Independently Expressing the *PPR-A* and *PPR-B* Genes

In order to analyze each of the three PPR proteins encoded by the radish *Rfo* locus, separate transgenic rapeseed lines expressing the corresponding genes were generated. This transgenic material was then used as an important resource for a comparative analysis of the three proteins and to provide functional data explaining why PPR-B is the only protein capable of suppressing the expression of *orf138* (Brown et al., 2003; Koizuka et al., 2003). The *PPR-A* and *PPR-B* genes have all the attributes required to encode functional and highly similar proteins. Predicted PPR-A and PPR-B proteins are 87% identical and 91% similar, but compared with PPR-B, PPR-A carries a 4–amino acid deletion in the third PPR repeat and a 66–amino acid C-terminal extension (Figure 1). By contrast, *PPR-C* is only predicted to encode a protein of similar size to PPR-B if a hypothetical intron is present to correct a frameshift mutation generated by a 17-bp deletion in roughly the middle of the gene (Desloire et al., 2003). To test this possibility, we sequenced an RT-PCR amplification product spanning this region of *PPR-C* but did not detect such an intron. Consequently, *PPR-C* is likely to encode a PPR protein half the size of PPR-B and thus is likely a pseudogene. For this reason, we did not generate any transgenic lines for this gene.

Genomic fragments carrying the *PPR-A* and *PPR-B* genes and their respective 5′ and 3′ regulatory regions were subcloned into the pEC2 binary vector and transformed into Ogu-INRA CMS rapeseed plants (Figure 2A). Six independent transgenic plants were obtained bearing the *PPR-A* construct and two bearing *PPR-B*. All of the *PPR-A* transgenic plants exhibited a male-sterile

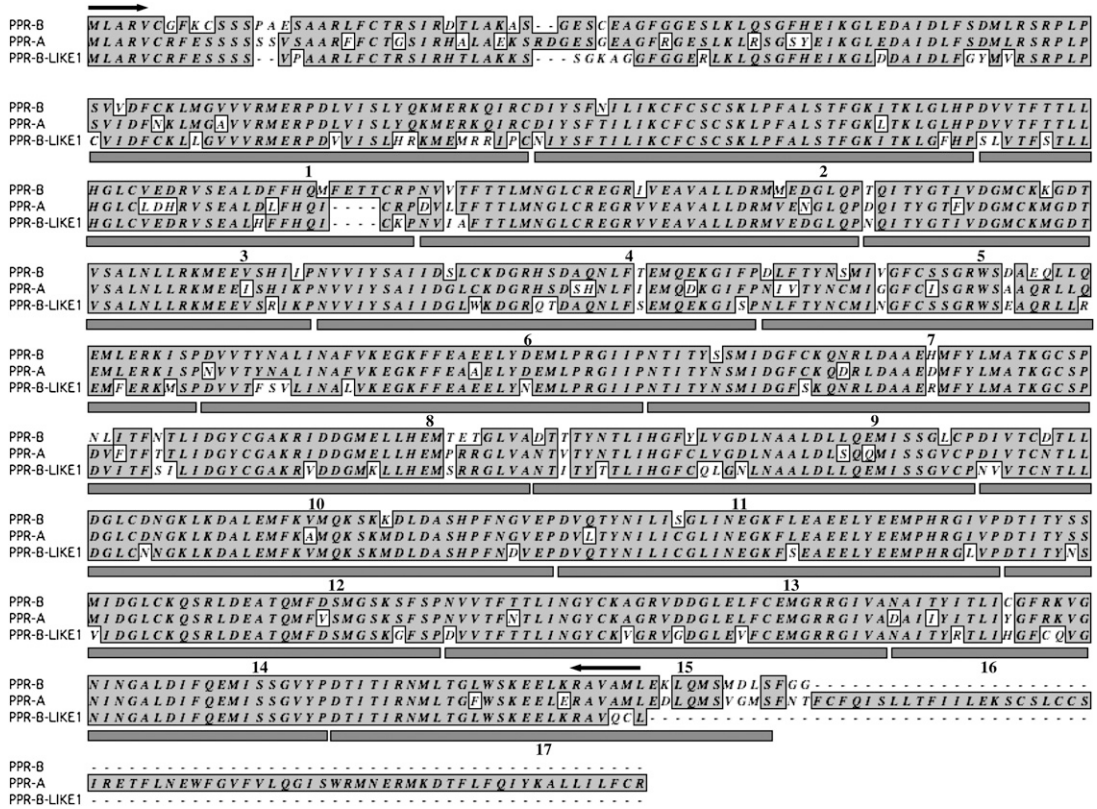

Figure 1. Protein Sequence Alignment of PPR-B and PPR-A from Radish and PPR-B-LIKE1 from Rapeseed.

Identical amino acids in all three sequences are boxed in gray, and gray shading indicates similar residues. The positions and numbers of PPR repeats are indicated underneath the protein sequences in gray boxes. The protein region located upstream of the first PPR repeat comprises the mitochondrial targeting sequence in each protein. The protein regions used to design PCR primers to amplify the *PPR-B-LIKE1* sequence from rapeseed are indicated with arrows.

phenotype, whereas the *PPR-B*–expressing lines were completely male-fertile (Figure 2B). The level of accumulation of both proteins in mitochondria was then estimated for each transgenic plant using a purified antiserum directed against the PPR-B protein (Figure 2C; see Supplemental Figure 1 online). The steady state level of the PPR-A protein appeared much lower than that of PPR-B in each transformed line. These results are only indicative of the relative abundance of each protein and are not strictly quantitative, although the anti-PPR-B antiserum has a similar sensitivity toward PPR-A and PPR-B (see Supplemental Figure 2 online). Two transgenic plants appeared to synthesize higher levels of PPR-A protein, correlating with an increased abundance of RNA expressed from the *PPR-A* transgene, than the four other transgenic lines (data not shown). These two lines (named A_1 and A_2) were retained for subsequent analyses. DNA gel blot analysis revealed that A_1 plants contained two copies of the transgene, whereas A_2 had only one insertion (Figure 3). Analysis of *PPR-B* transgenic lines indicated that the first line (B_1) contained four insertions, whereas the second line (B_2) carried only one copy of the transgene (Figure 3). Accordingly, segregation analysis of selfed or backcrossed plants showed that restoration was controlled by a single locus from the B_2 parent, whereas segregation of this trait was more complex for B_1 plants. The higher transgene copy number in the B_1 compared with the B_2 line correlated with an apparent higher level of PPR-B accumulation (Figure 2C). The B_1 transgenic line was thus selected for further analyses.

Several cross-hybridizing bands were observed on DNA gel blots with *PPR-A*– and *PPR-B*–specific probes, even when probing DNA from untransformed plants (S genotype in Figure 3B). We reasoned that these bands may correspond to endogenous rapeseed genes showing significant homology to *PPR-A* and *PPR-B* genes. Some of these may encode proteins similar in size to PPR-B, as a faint cross-reacting signal was systematically detected around 70 kD by the anti-PPR-B antibodies when using mitochondrial extracts prepared from untransformed plants (Figure 2B). To identify one or more of these genes, a pair of primers was designed based on the highly conserved 5′ and 3′ extremities of *PPR-A* and *PPR-B* (Figure 1). A single PCR product of around 2 kb was amplified from rapeseed DNA, which was cloned and subsequently sequenced. All of the clones contained DNA inserts corresponding to the same gene and encoded a putative protein fragment sharing 83% identity (91% similarity) with PPR-B (Figure 1). Interestingly, like PPR-A, this rapeseed protein carries a short deletion in the third PPR repeat. This gene, which encodes a protein without restoration activity toward the Ogu-INRA CMS, was named *PPR-B-LIKE1*.

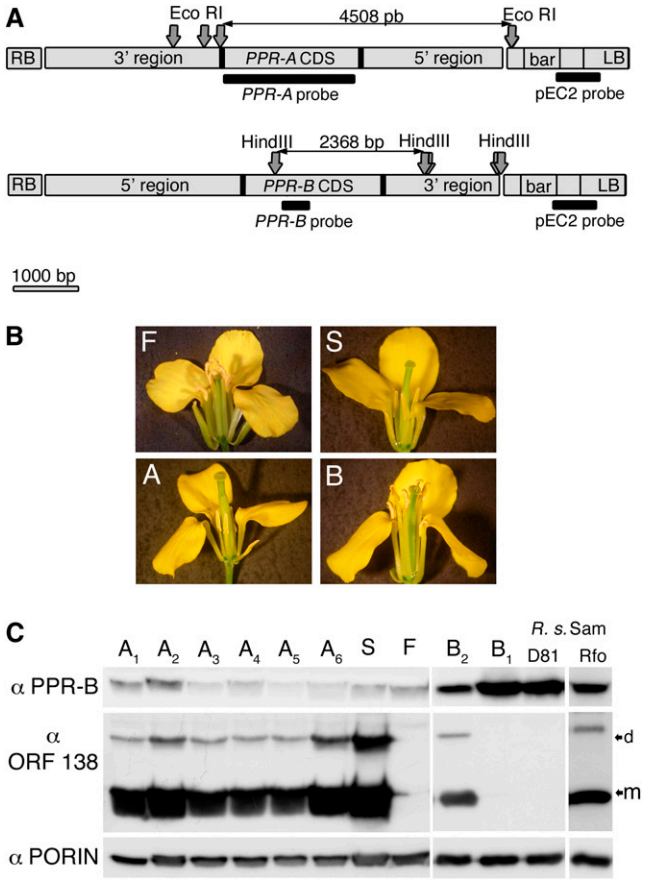

Figure 2. Phenotypic and Molecular Characterization of Rapeseed Transgenic Plants Independently Expressing the *PPR-A* or *PPR-B* Genes from Radish.

(A) Schematic representation of the transgenes used to transform Ogu-INRA CMS rapeseed plants. The promoter (5′ region), the coding sequence (*PPR-A* CDS or *PPR-B* CDS), the terminator (3′ region), and the basta resistance gene (bar) used for selection are indicated in gray boxes. The *Eco*RI and *Hin*dIII restriction sites and the different transgene fragments used as probes are indicated with arrows and horizontal bars, respectively. LB, T-DNA left border; RB, T-DNA right border.

(B) Partially dissected rapeseed flowers showing anther morphology and pollen production from plants of the indicated genotype. F, male-fertile plant; S, Ogu-INRA CMS plant; A, example of an Ogu-INRA CMS plant transformed with *PPR-A*; B, example of an Ogu-INRA CMS plant transformed with *PPR-B*.

(C) Protein gel blot analysis showing the level of accumulation of PPR-A, PPR-B, and ORF138 proteins in different rapeseed transgenic plants in comparison with reference rapeseed and radish restored lines. Fifty micrograms of total mitochondrial protein preparations was separated on SDS-polyacrylamide gels, transferred to polyvinylidene fluoride membranes, and probed with anti-PPR-B, anti-ORF138, or anti-PORIN antibodies, as a loading control. Specific signals corresponding to ORF138 monomers (m) or dimers (d) are indicated by arrows at right. A_1 to A_6 plants correspond to the six *PPR-A* transgenic plants obtained, and B_1 and B_2 correspond to the two plants expressing the *PPR-B* transgene. SamRfo corresponds to a reference restored rapeseed line carrying a large DNA introgression from radish comprising the entire *Rfo* locus, and the sample termed R.s.D81 was obtained from the restored D81 radish line. The extracts annotated S and F correspond, respectively, to the male-sterile and male-fertile plants shown in **(B)**.

Correlations between *PPR-A*, *PPR-B*, and *orf138* Expression Levels in Flower Bud Tissues

To investigate the relationship between the phenotypes of the transgenic plants and the degree to which ORF138 synthesis was affected, we monitored the steady state levels of the sterility protein in mitochondria from each genotype. As expected, due to their male-sterile phenotype, ORF138 expression in mitochondria from plants expressing *PPR-A* was indistinguishable from that of untransformed control plants (Figure 2C). Interestingly, the high level of PPR-B synthesis in the B_1 transgenic line correlated with the almost complete elimination of the ORF138 protein (Figure 2C). ORF138 expression, however, showed a more moderate decrease in the B_2 line, even though the plant was completely male-fertile (Figure 2C). Furthermore, analysis of reference (and nontransgenic) restored lines indicated that, in the B_1 line, ORF138 suppression was comparable to that in the D81 restored radish line (Desloire et al., 2003). By contrast, ORF138 suppression by *PPR-B* in the B_2 line was similar to that seen in the SamRfo rapeseed line, which carries a large DNA introgression from radish comprising the entire *Rfo* locus (Figure 2C) (Delourme et al., 1998; Giancola et al., 2003).

As *Rfo* was previously shown to suppress ORF138 accumulation in a tissue- and development-specific manner, the regulation of *PPR-B* expression and its effects on ORF138 accumulation were evaluated (Krishnasamy and Makaroff, 1994; Bellaoui et al., 1999). Initially, the levels of PPR-A, PPR-B, and ORF138 synthesis were examined in protein extracts prepared from young developing flower buds of sizes increasing from 1 to 3 mm. For each developmental stage, anthers were dissected from buds and proteins were prepared from isolated anthers and from emasculated flowers. In both transgenic lines tested, PPR-A appeared to accumulate at slightly higher levels in anthers from 1-mm buds, although the low levels of PPR-A made the comparison difficult (Figure 4A). The ORF138 levels in these lines did not differ from those in untransformed male-sterile control plants in any of the tissues and developmental stages tested. By contrast, PPR-B accumulated at much higher levels in anthers compared with other floral tissues, with a slight peak in anthers isolated from 1-mm buds (Figure 4A). The subsequent decrease in ORF138 synthesis was very pronounced and appeared to be homogenous across the different tissues and developmental stages tested for this line, indicating that even relatively low levels of PPR-B can lead to a dramatic decrease in ORF138, as seen in the samples corresponding to buds with their anthers removed. The same analysis was also performed on the SamRfo restored rapeseed, because this line accumulates higher levels of ORF138 than the B_1 transgenic line and we wanted to see whether this difference is limited to certain types of plant/floral tissues. In this line, the antagonistic effect of PPR-B on ORF138 synthesis also appeared stronger in anthers than in the remaining floral tissues, but suppression of ORF138 synthesis was globally less pronounced than that in the B_1 transgenic line (Figure 4B). These results indicate that the B_1 transformed line

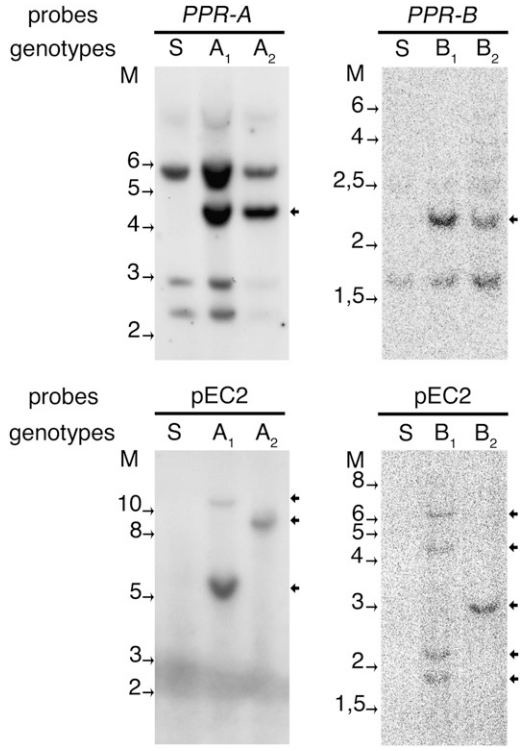

Figure 3. DNA Gel Blot Analysis of Transgenic Rapeseed Plants Expressing Either *PPR-A* or *PPR-B*.

Total DNA from untransformed (S) or transgenic lines transformed with *PPR-A* (A_1 and A_2) or *PPR-B* (B_1 and B_2) were digested with *Eco*RI or *Hin*dIII, respectively, prior to being blotted and hybridized with the probes indicated in Figure 2A. Arrows at right indicate hybridization signals specific to the transgenes. Molecular size markers are included at left.

expressed higher levels of PPR-B compared with the SamRfo line, likely because of the presence of several copies of the *PPR-B* gene in its genome. To test whether *PPR-B* was still subjected to the same type of regulation of expression in the B_1 line, the abundance of PPR-B in other plant tissues was determined (Figure 4C). The highest levels of PPR-B accumulation seemed to occur in flower buds smaller than 3 mm, as a weaker signal was detected in larger buds. Hardly any signal was detected in leaf and root protein extracts, although sufficient levels of PPR-B protein were again produced to inhibit the synthesis of ORF138 almost completely in these tissues. In conclusion, our B_1 transformed line accumulated higher levels of the restorer protein, but the overall regulation of expression of the gene was maintained, as demonstrated by the elevated accumulation of PPR-B in young reproductive tissues.

Immunolocalization of ORF138 in Rapeseed Anther Sections

Previous studies established that ORF138-triggered sterility was linked to premature degeneration of the tapetal cell layer during pollen development, leading to the collapse of microspores (Gourret et al., 1992). Since *PPR-B* expression appeared to be tissue-specific, the corresponding effect of PPR-B on the amount of ORF138 accumulation in the tapetal cell layer was examined. Immunolocalization of ORF138 was performed on bud sections of 1- to 2-mm flowers, the developmental stage that showed the highest level of *PPR-B* expression (Figure 4A). The ORF138 protein was found to accumulate throughout the anther loculi of male-sterile genotypes (Sam and Fu58 in Figure 5), appearing as punctate signals similar to those produced by the anti-PORIN control antibodies (Figure 5). The ORF138 protein was also detected at high levels in young microspores. Although *PPR-A* expression had no real effect on the accumulation of sterility protein, both plant lines expressing the *PPR-B* gene contained much lower amounts of ORF138. No ORF138 signal at all was detected in the B_1 transgenic line (Figure 5). In the SamRfo line, however, trace amounts of the sterility protein were still detected in anthers, but interestingly, ORF138 appeared to be totally absent in the tapetum (Figure 5).

These results indicated that complete elimination of the ORF138 protein in the tapetal cell layer correlates with the restoration of fertility and confirmed that the B_1 transgenic line obtained in this study shows almost complete suppression of ORF138 in all anther tissues. We attempted to corroborate these data by localizing the PPR-B protein on the anther sections, but a specific signal could not be obtained with the anti-PPR-B antibodies.

In Situ Localization of *orf138* mRNA

Previous investigations of the molecular events underlying fertility restoration suggested that suppression of the sterility-inducing protein was not correlated with changes in the size or amount of the *orf138* transcript (Bellaoui et al., 1999). These previous conclusions were made from the analysis of heterogeneous samples containing various kinds of tissues, and the approaches used could not completely exclude the possibility that some cell- or tissue-specific degradation of the *orf138* mRNA had occurred. The results of our immunolocalization study (Figure 5) suggested that tissue-specific effects may be taking place, since loss of ORF138 through the action of *PPR-B* appeared to be partial outside the tapetum in the SamRfo-restored plants, which were previously used to analyze the fate of *orf138* mRNA in restored tissues (Bellaoui et al., 1999). Thus, in situ hybridization experiments were conducted on 1- to 2-mm flower bud sections to determine the amount of *orf138* mRNA in reproductive tissues of various genotypes (Figure 6). Strong and specific hybridization signals were visualized in all cell types of anthers of sterile plants, including those expressing *PPR-A* (Fu58, S, and A samples in Figure 6). The most intense signals were observed in the tapetal cells and tetrads, which may simply reflect the higher content of active mitochondria in these cell types. However, the restored genotypes showed no quantitative decrease in *orf138* hybridization signals, suggesting that the action of *PPR-B* does not result in a dramatic reduction in *orf138* mRNA, even in a cell-specific manner.

The PPR-B Protein Is Both a Soluble and a Membrane-Associated Mitochondrial Protein

Targeting of PPR-B to the mitochondria was initially verified by creating a C-terminal green fluorescent protein fusion encompassing the first 44 amino acids of the protein, which targeted

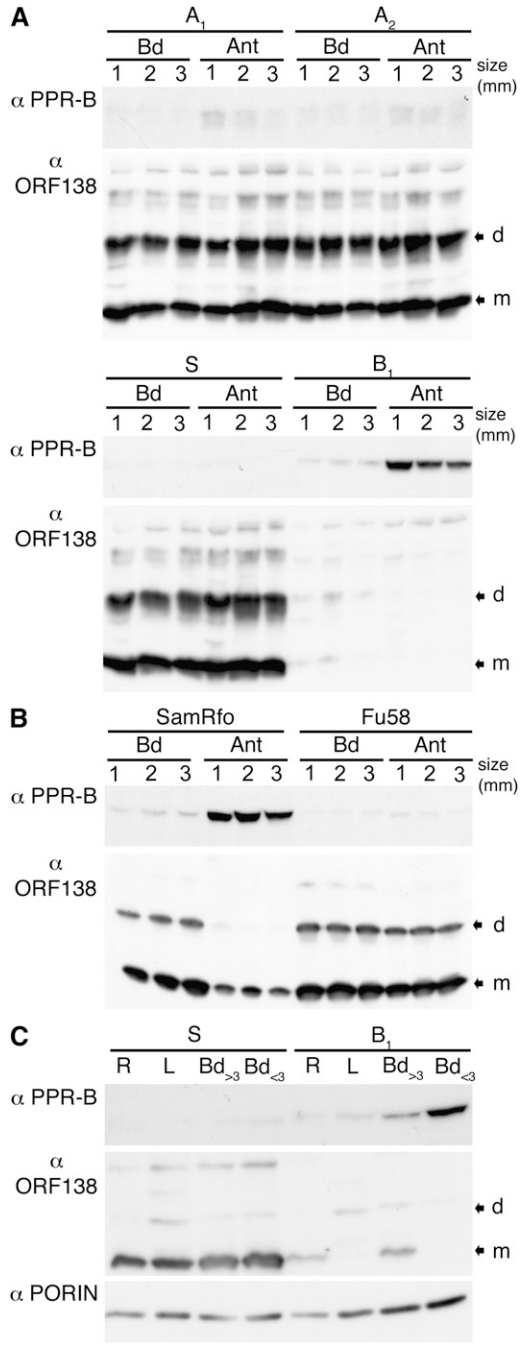

Figure 4. PPR-A and PPR-B Proteins Accumulate Preferentially in the Anthers of Young Floral Buds.

The protein gel blots shown were probed with either the anti-PPR-B or anti-ORF138 antibody, as indicated.

(A) Analysis was performed using total protein preparations obtained from dissected flower buds 1, 2, or 3 mm in size. As indicated, two kinds of tissues were distinguished: isolated anthers (Ant) and flower buds from which anthers were removed (Bd). A_1, A_2, S, and B_1 samples correspond to the same genotypes presented in Figure 2. Specific signals corresponding to ORF138 monomers (m) or dimers (d) are indicated by arrows at right.

mitochondria when transiently expressed in tobacco (*Nicotiana benthamiana*) leaves (see Supplemental Figure 5 online). The cellular distribution of PPR-B was further analyzed by probing total, chloroplastic, and mitochondrial protein preparations from the B_1 transgenic line with the anti-PPR-B antibody. PPR-B was strongly enriched in isolated mitochondria, as shown by antibodies to marker proteins NAD9 (for subunit 9 of mitochondrial NADH dehydrogenase) and ATPC (for γ-subunit of plastid ATP synthase) (Figure 7A). The submitochondrial distribution of the restorer protein was then investigated (Figures 7B and 7C). Following a lysis step, mitochondrial extracts were fractionated for soluble and membrane proteins. The PPR-B protein appeared to be approximately equally distributed between soluble and membrane protein fractions (Figure 7B). Several lysis procedures were tested, some of which did not lead to mechanical breaking of mitochondrial membranes, and PPR-B was always found to be associated with the soluble protein fraction. This suggests that the restorer protein may exist both as a soluble and as a membrane-bound protein or that the protein is loosely attached to mitochondrial membranes. The mitochondrial membrane fraction was subsequently subjected to sodium carbonate treatment, which reportedly solubilizes extrinsic membrane proteins (Fujiki et al., 1982). Unlike NAD9 and RPL12, PPR-B was extracted less efficiently from membranes under these conditions (Figure 7C). Our results suggest that PPR-B distribution is rather unusual, as it appears to be a soluble mitochondrial protein but also associates tightly with mitochondrial membranes. The nature and topology of this association remain to be clarified.

PPR-B Associates with the *orf138* Transcript in Vivo

A number of PPR proteins were reported to associate in vivo or in vitro with the RNA of their cognate organelle target gene (Nakamura et al., 2003; Schmitz-Linneweber et al., 2005, 2006; Gillman et al., 2007; Beick et al., 2008; Kazama et al., 2008; Williams-Carrier et al., 2008). To investigate whether this kind of interaction occurs between PPR-B and *orf138* mRNA, immunoprecipitation experiments were performed with anti-PPR-B antibodies, using mitochondrial extracts from *PPR-A*– and *PPR-B*–transformed lines as well as from control untransformed plants. RNA was then extracted from both supernatants and immunoprecipitation pellets, slot-blotted onto membranes, and analyzed with different DNA probes. The hybridization signals for each probe were quantified, and ratios between pellet and supernatant measurements were calculated to detect specific enrichment of particular RNA species within immunoprecipitates, as

(B) Identically treated protein samples derived from two rapeseed lines of the Samouraï variety. The Fu58 line corresponds to Ogu-INRA CMS plants, cv Samouraï, and SamRfo is the associated restored line carrying a large genomic introgression from radish comprising the entire *Rfo* locus and the three PPR genes.

(C) Total protein preparations obtained from roots (R), leaves (L), floral buds between 0 and 3 mm in size (Bd < 3), and buds larger than 3 mm (Bd > 3) of restored (B_1) and sterile (S) plants were analyzed with anti-PPR-B, anti-ORF138, or anti-PORIN antibodies as a loading control.

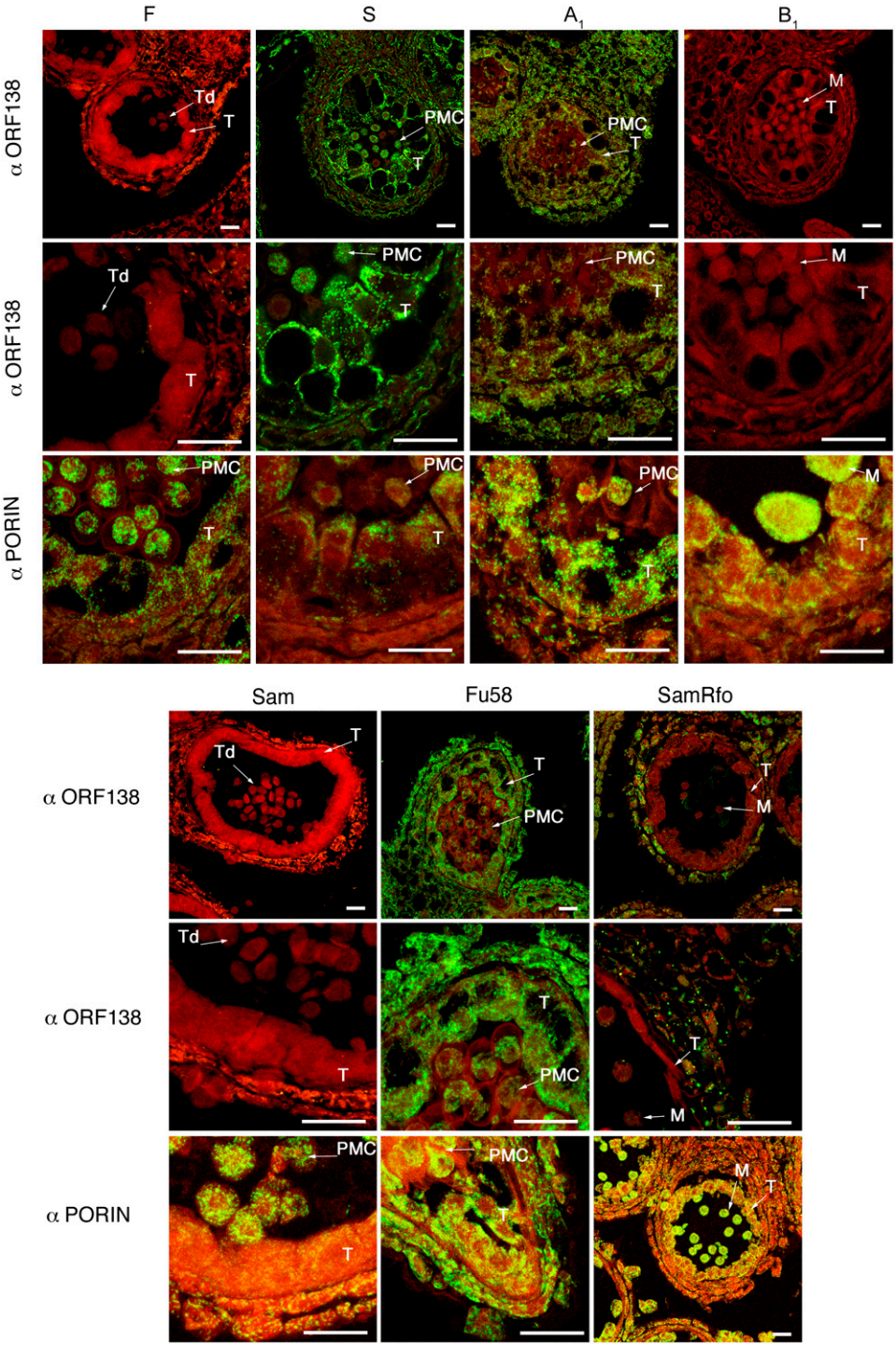

Figure 5. The Major Role of *PPR-B* Is to Prevent the Accumulation of ORF138 in the Tapetum of Anthers.

Confocal microscopy views of young anther sections labeled with either the anti-ORF138 (αORF138) or the anti-PORIN (αPORIN) antibody. Specific hybridization signals generated by these antibodies appear as green spots whose size and distribution resemble mitochondria. The images in the middle row are enlargements of the top row of images. The anther sections annotated F, S, A_1, B_1, Fu58, and SamRfo correspond to the plant genotypes described in Figures 2 and 4B, whereas the Sam sample corresponds to cv Samouraï male-fertile plants. M, microspores; PMC, pollen mother cells; T, tapetal cell layer; Td, tetrad of microspores. Bars = 20 μm.

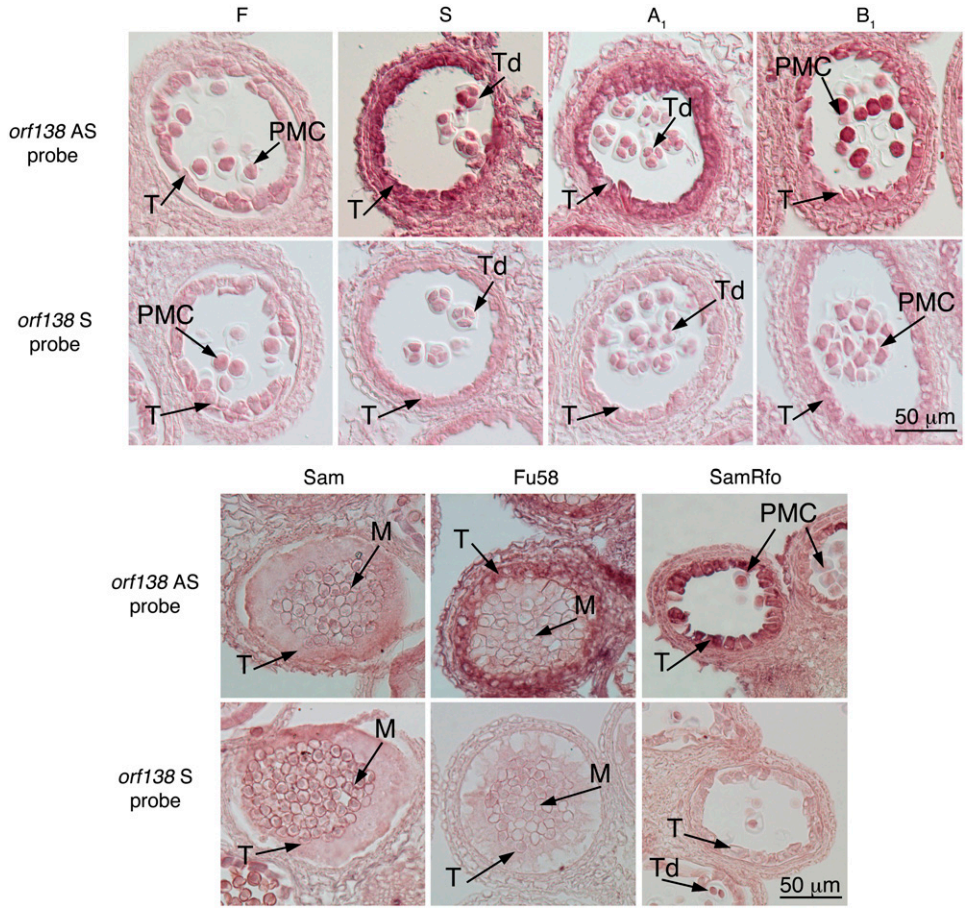

Figure 6. *PPR-B* Does Not Affect the Local Accumulation of *orf138* mRNA in Young Anthers.

In situ hybridization performed with *orf138* sense (S) and antisense (AS) probes on sections of anthers made from 2- to 3-mm flower buds. Specific signals are dark pink. The various genotypes tested are identical to those in Figure 5. Arrows indicate various anther structures. M, microspores; PMC, pollen mother cells; T, tapetal cell layer; Td, tetrad of microspores. Bars = 50 μm.

reported previously in similar studies (Schmitz-Linneweber et al., 2005, 2006). Although the anti-PPR-B antiserum successfully immunoprecipitated the PPR-B protein from mitochondrial extracts obtained from plants transformed with *PPR-B* (B_1), a signal of similar intensity was also obtained in untransformed controls (S) and plants transformed with *PPR-A* (A_1), suggesting that PPR-B–related proteins, such as PPR-B-LIKE1 or PPR-A, are also efficiently immunoprecipitated by the antiserum (Figure 8A). Analysis of the hybridization signals showed that *orf138* RNA was specifically enriched in the immunoprecipitated pellet from *PPR-B*–expressing plants. Much weaker signals, and corresponding relative enrichments of the *orf138* RNA, were detected in pellets generated from S and A_1 mitochondrial extracts (Figures 8B and 8C). By contrast, *cox2* and *atp1* RNAs, which are not involved in fertility restoration, did not significantly coimmunoprecipitate with PPR-B. Similarly, no equivalent enrichments of the *orf138* RNA were observed when an antiserum other than anti-PPR-B was used (Figures 8B and 8C). These results indicate that PPR-B associates with the *orf138* RNA in vivo, unlike PPR-A and other PPR-B–related proteins expressed in rapeseed.

DISCUSSION

PPR-B Homologs and Expression Patterns

The cloning of *Rf* genes in petunia, radish, and rice has demonstrated that fertility restoration loci often contain several very similar PPR genes arranged in tandem, among which a single gene generally confers the actual restoration function. The Ogura restorer locus contains three highly related genes, arbitrarily named *PPR-A*, *PPR-B*, and *PPR-C* (Desloire et al., 2003). The driving forces behind this genomic organization remain poorly understood, but this characteristic singles out restorer genes as a particular class of PPR genes that undergo extremely active duplications, in a similar way to pathogen-resistance genes in plants (Richter and Ronald, 2000; Geddy and Brown, 2007). Here, we conducted a comparative analysis of the PPR genes present at an *Rf* locus in radish. One of the objectives was to identify key functional differences between the different members of this cluster to help understand why PPR-B is the only encoded protein that has been genetically demonstrated to

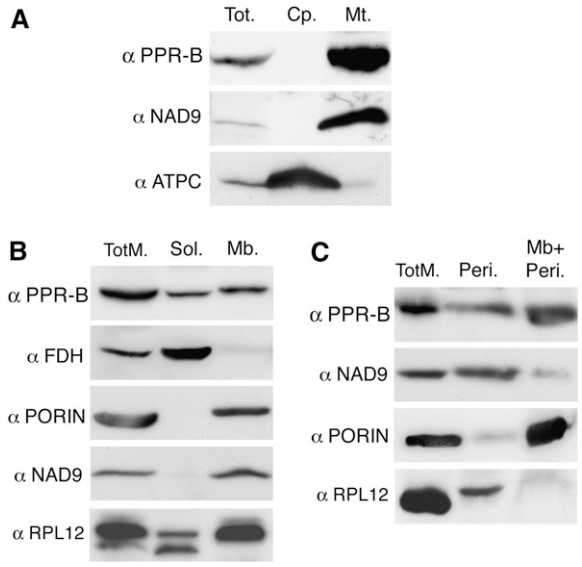

Figure 7. Analysis of the Submitochondrial Location of PPR-B.

(A) Analysis of total (Tot.), chloroplast (Cp.), and mitochondrial (Mt.) protein preparations from the B_1 transgenic line. Antibodies to marker proteins NAD9 and ATPC were used to verify the correct purification of mitochondria and chloroplasts, respectively.

(B) Assessment of proteins present in total mitochondrial protein preparation (TotM.) and in soluble (Sol.) and membrane (Mb.)–derived protein fractions. Protein gel blots were labeled with anti-PPR-B antibodies (α PPR-B); anti-formate dehydrogenase (α FDH), which detects a known soluble matrix protein; anti-mitochondrial PORIN (α PORIN), which detects an integral membrane protein of the outer mitochondrial membrane; anti-NAD9 (α NAD9), an extrinsic protein of the inner membrane of mitochondria; and anti-RPL12 (α RPL12), a ribosomal protein that is both soluble and extrinsically associated with the inner membrane of mitochondria. All samples were prepared from mitochondria purified from B_1 transgenic plants. Each lane was loaded with ~25 μg of proteins.

(C) Analysis of the protein content of sodium carbonate–treated mitochondrial membranes. Purified mitochondrial membranes were treated with sodium carbonate to release and solubilize peripheral membrane proteins (Peri.). Proteins of the Mb+Peri. sample correspond to proteins that were incompletely solubilized (such as extrinsic membrane proteins) or insoluble (such as integral membrane proteins) by the sodium carbonate treatment. Approximately 25 μg of each protein preparation was loaded onto each lane, and blots were probed with the indicated antibodies.

restore fertility. To this end, transgenic rapeseed plants independently expressing two of the different *Rfo* locus *PPR* genes from radish were produced. The *PPR-C* gene was omitted from the study because analysis of cDNA sequences indicated that it is a pseudogene. By examining the transgenic material generated, we confirmed that, as previously reported, *PPR-A* does not restore fertility, unlike *PPR-B* (Figure 2) (Brown et al., 2003; Koizuka et al., 2003). However, *PPR-A* was also shown to be an active gene, and the PPR-A protein, like PPR-B, accumulated preferentially in young anthers, although at low levels (Figure 4). We also observed that PPR-A was hardly detectable in both total and mitochondrial extracts, in contrast with PPR-B, which accumulated at much higher levels (Figure 3). Differences in transcriptional activities of *PPR-A* and *PPR-B* genes, in the translational efficiency of mRNAs, or in the stability of encoded proteins may explain these differences, which may be related to different cellular functions of *PPR-A* and *PPR-B* or, alternatively, may suggest that *PPR-A* is inactive and represents a degenerate duplication of *PPR-B*.

A faint band, the same size as PPR-B, was observed using the anti-PPR-B antibody on untransformed plant extracts, which led us to believe that the rapeseed genome may also encode one or several proteins highly homologous to PPR-B. Similar bands were also visible on DNA gel blots from transformed and untransformed rapeseed plants, as *PPR-A*– and *PPR-B*–specific probes revealed three or four bands in addition to the signals specific to each transgene. We used a simple PCR-based approach to determine the sequence of one of these genes, named *PPR-B-LIKE1*, whose encoded protein shares 86% and 87% identity with PPR-B and PPR-A, respectively. Many differences distinguish PPR-B-LIKE1 from PPR-B, although it is interesting that PPR-B-LIKE1 shares the same four–amino acid deletion in its third PPR repeat as PPR-A, which therefore may be deleterious for the restoration function. Besides *PPR-A* and *PPR-C*, *PPR-B-LIKE1* represents a third close homolog of *PPR-B* and expands the sequence data available on the *PPR-B*–related genes. This novel sequence indicates that *PPR-B*–like genes are not restricted to the *Raphanus* genus and originated from ancestral genes present in the founders of the Brassicaceae family. Several genes homologous to *PPR-B* have been identified in the *Arabidopsis* genome, although no strict ortholog of *PPR-B* has been identified in the genomic region syntenic to the *Rfo* locus (Brown et al., 2003; Desloire et al., 2003; Geddy and Brown, 2007). It would thus appear that *PPR-B* evolved in response to the Ogura CMS and derived from a reservoir of *PPR-B*-like genes, which seems to be a relatively common class of PPR genes in the Brassicaceae genome. It will be interesting to determine the role played by some of the *PPR-B*–like proteins, if they are active, and to understand from what kind of function the Ogura CMS fertility restorer gene has evolved. Restorer-like PPR genes thus appear to be a particular class of PPR genes that evolve rapidly and represent a molecular arsenal for the nucleus to use in response to the appearance of CMS genes and perhaps other kinds of mitochondrial alterations. This type of adaptation is reminiscent of that observed for disease-resistance loci (Touzet and Budar, 2004; Geddy and Brown, 2007).

The Removal of ORF138 from the Tapetum of Anthers Appears to Be Crucial for the Restoration of Male Fertility

Immunolocalization of the ORF138 protein in young anther sections indicated that the sterility protein accumulates at high levels in male-sterile lines, without showing any increase in any particular anther tissues. All of the restored lines showed a drastic decrease in the ORF138 signal, but the level of inhibition appeared to vary between the different lines tested. The SamRfo rapeseed line, which contains a single copy of *PPR-B* on a large DNA region introgressed from radish (Delourme et al., 1998; Giancola et al., 2003), shows a nonhomogenous decrease in ORF138 synthesis in anther tissues. The sterility protein only

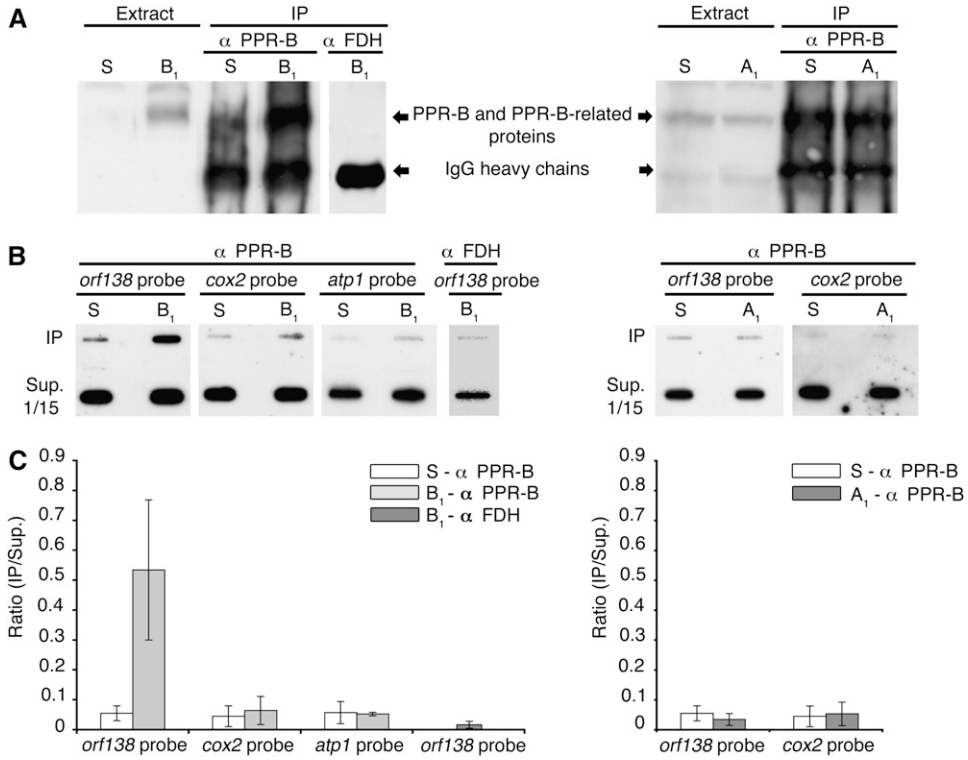

Figure 8. *orf138* mRNA Coimmunoprecipitates with PPR-B from Mitochondrial Extracts.

Clarified mitochondrial extracts prepared from rapeseed plants of the indicated genotypes were immunoprecipitated with the affinity-purified anti-PPR-B antibody or an anti-FDH antibody, as indicated. The three genotypes tested (S, B_1, and A_1) are identical to those in Figure 2.

(A) Immunoblot analysis of initial mitochondrial lysis extracts (Extract) and immunoprecipitates (IP) to verify the immunoprecipitation of PPR-A (A_1), PPR-B (B_1), and PPR-B–related proteins (S) by the anti-PPR-B antibody (α PPR-B) but not by the anti-FDH antibody (α FDH). PPR-A and PPR-B are from radish, and the PPR-B–related proteins are from rapeseed.

(B) Analysis of RNA content in immunoprecipitates and supernatants. RNA corresponding to the experiments presented in **(A)** was extracted from the immunoprecipitate pellets (IP) and one-fifteenth of supernatants (Sup. 1/15) and slot-blotted onto a nylon membrane. Blots were hybridized with *orf138*-, *cox2*-, or *atp1*-specific probes, as indicated.

(C) Quantification of hybridization results. Hybridization signals obtained from one-fifteenth of the supernatant and immunoprecipitates for each probe were quantified with a BAS5000 phosphor imager (Fuji). Immunoprecipitate-to-supernatant signal (IP/Sup.) ratios are presented for each probe (*orf138*, *cox2*, and *atp1*), genotype (S, A_1, and B_1), and antibody used (α-PPR-B and α-FDH). Error bars correspond to SD calculated after three experimental repeats.

completely disappeared in tapetal cells and microspores, with weak but significant amounts of ORF138 detected in other anther tissues (Figure 5). The partial effect of *PPR-B* in the SamRfo revealed that its principal sites of action reside in tapetal cells and microspores, which also correlated with increased synthesis of the restorer protein in developing anthers (Figure 4). *PPR-B* regulatory DNA elements, therefore, likely evolved to maximize the production of the restorer protein in tissues that are critical for pollen production. Indeed, the tapetum plays a nutritive role for microspores and is involved, among other things, in callase production to release the young haploid microspores from the callose wall enclosing the meiotic tetrads (Bedinger, 1992). Our results suggest that the complete removal of ORF138 from the tapetum and microspores is likely to be essential for the molecular events leading to restoration. This is consistent with observations showing that the Ogura CMS was associated with developmental defects in these two cell types. Premature vacuolization and death of the tapetum at the end of meiosis, followed by microspore degeneration after reaching the vacuolated stage, have been linked to the expression of ORF138 (Gourret et al., 1992). These observations were recently correlated with abnormal mitochondrial structures in tapetal cells and vacuolated microspores (González-Melendi et al., 2008). It is not clear how these two developmentally separated events are physiologically connected or which event is most responsible for the CMS phenotype. However, the sporophytic nature of *PPR-B*–driven fertility restoration indicates that the maintenance of a functional tapetum by eliminating ORF138 is sufficient for fertility restoration. Consequently, tapetum dysfunction appears to be the initial event leading to CMS, through the abortion of microspores later in development. Our observation that ORF138 disappears from the tapetal cell layer in response to *PPR-B* supports these conclusions.

Unlike SamRfo, the B_1 transgenic line obtained in this study showed almost complete disappearance of ORF138 in the various anther tissues. Surprisingly, ORF138 disappearance in

this line was not limited to male reproductive tissues and occurred in most parts of the plant. The B_1 transgenic line, which carries four copies of the transgene, had higher overall expression of *PPR-B* than SamRfo, but expression appears to have remained tissue-specific, with higher levels in anthers compared with other plant tissues, as was also seen in the SamRfo line.

PPR-B Specifically Associates with *orf138* RNA in Vivo, Unlike Other PPR Family Members

The PPR-B sequence is entirely constituted of PPR repeats, suggesting that, among likely functions attributable to the restorer protein, those involving the fate of the *orf138* mRNA were the most plausible. Indeed, genetic characterization of PPR mutants showed that most affect the biogenesis of specific RNA species, in many different ways. Additionally, several other nuclear restorers are thought to mediate the processing or translation of CMS-associated transcripts (Hanson and Bentolila, 2004; Chase, 2007). Previous studies on *Rfo* proposed that *PPR-B* is implicated translationally or posttranslationally in the synthesis of ORF138, because a single stable mRNA species accumulated in both sterile and restored plants (Krishnasamy and Makaroff, 1994; Bellaoui et al., 1999). However, these studies analyzed RNA or protein in preparations obtained from tissues in which the action of *Rfo* was probably not homogeneous, as we observed in the SamRfo line. Therefore, although potential local actions by *PPR-B*, for instance on the stability of the *orf138* mRNA, could have been missed, our in situ hybridization results showed that, at the tissue level, *PPR-B* does not appear to be involved in the local degradation of *orf138* mRNA, like in the tapetum for instance (Figure 6).

Using the transgenic restored B_1 line, in which the action of *PPR-B* is close to homogeneity, we examined the in vivo association between PPR-B and the *orf138* mRNA. We found that *orf138* mRNA coimmunoprecipitates with the restorer protein, suggesting that PPR-B makes direct or indirect contacts with the *orf138* mRNA (Figures 8B and 8C). Interestingly, this was not the case for PPR-A or any of the PPR-B–like proteins in rapeseed, which were also immunoprecipitated by our anti-PPR-B antiserum (Figures 8B and 8C). These results link genetic and molecular data and suggest that nonrestoring proteins cannot support the function of restoration, possibly because they cannot directly or indirectly associate with the *orf138* mRNA. If a lack of association with the *orf138* mRNA is the only reason why a maintainer does not restore fertility, an interesting evolutionary scenario can be proposed in which PPR-B has evolved toward the function of restoration by acquiring an ability to bind to a precise region of the *orf138* mRNA. The *orf138* mRNA binding potential may be essential to achieve restoration, although it cannot be excluded that the ability to direct subsequent molecular events may also be fundamental to the inhibition of ORF138 production. Without yet knowing which part of the *orf138* mRNA is targeted by PPR-B, it is difficult to make conclusions regarding the mode of action of PPR-B. Nevertheless, our results favor a role for *PPR-B* in the translational control of the *orf138* mRNA and provide less support for *PPR-B* directing ORF138 to proteolysis, as proposed previously (Bellaoui et al., 1999). Our current view on PPR-B action is that it can specifically impair ORF138 protein synthesis by preventing *orf138* mRNA translation by mitochondrial ribosomes. PPR-B could associate with the 5′ untranslated region (UTR) of the *orf138* mRNA and consequently prevent either the attachment or the progression of the mitochondrial translation machinery. Although the 5′ UTR of the *orf138* transcript is partially homologous to the 5′ UTR of the *atp6* mRNA present in normal radish cytoplasm (Krishnasamy and Makaroff, 1994), the copy of *atp6* present in sterile cytoplasm has a different 5′ UTR (Krishnasamy and Makaroff, 1994); thus, this *atp6* sequence may have evolved to escape from the inhibitory control of PPR-B. Additional efforts will be necessary to confirm this model and verify that PPR-B binds to the 5′ UTR of the *orf138* mRNA. The product of the petunia *Rf592* gene was recently shown to associate with the 5′ UTR of the petunia *pcf* transcript (Gillman et al., 2007). It is possible that Rf592 affects the production of PCF in a similar way to the model we proposed for PPR-B, although it is also thought to mediate processing of the *pcf* transcript. Recently, the *Rf1* gene product was also suggested to reduce polysome association of the mRNA encoding the sterility protein in the BT-type CMS of rice (Kazama et al., 2008). Nevertheless, in contrast with PPR-B, translational reduction of the *orf79* mRNA is likely not a direct effect of *Rf1* but is secondary to *atp6-orf79* cotranscript processing.

We also determined the submitochondrial localization of PPR-B (Figure 7). PPR-B was found in the soluble mitochondrial protein fraction but was also associated with membranes. This association was only partially sensitive to high-pH treatment (Figure 7C), suggesting that the presence of PPR-B among soluble proteins was not a consequence of a weak and extrinsic membrane association. Further studies are needed to determine whether PPR-B is present at more than one location inside mitochondria. Most PPR proteins characterized so far were found to be soluble proteins, although the yeast petite 309 protein, the *Arabidopsis* pentatricopeptide repeat 336 protein, and the petunia restorer protein Rf592 showed fractionation patterns indicating an association with the mitochondrial inner membrane (Krause et al., 2004; Gillman et al., 2007; Uyttewaal et al., 2008). Whether the association of PPR-B with mitochondrial membranes is important for its activity remains to be determined. However, an interaction between PPR-B and the *orf138* mRNA could be revealed by coimmunoprecipitation only when adding Triton to the mitochondrial lysis buffer (Figures 8B and 8C), suggesting that the detergent allowed extraction of PPR-B/*orf138* mRNA complexes from membranes. We may thus speculate that only the membrane-associated fraction of PPR-B makes direct or indirect contacts with the *orf138* mRNA. The membrane association of PPR-B could also be mediated by bicistronic *orf138-orfB* mRNA, which may be recruited to the inner membrane by specific *orfB* translational activators, as described for several yeast mitochondrial mRNAs (Fox, 1996).

METHODS

Plant Material

The *PPR-A* and *PPR-B* genes were isolated by restriction digestion from the previously described BAC 64 (Desloire et al., 2003). A *Bgl*II restriction fragment of 7187 bp containing the *PPR-A* gene was subcloned into the

unique *Bam*HI site of the pEC2 binary vector (Cartea et al., 1998). A 7169-bp *Spe*I digestion fragment containing *PPR-B* was first subcloned into a modified pBluescript SK+ vector (Stratagene) containing two *Not*I sites and subsequently transferred into pEC2 at the *Not*I site. Both constructs were used to transform Ogu-INRA CMS rapeseed (*Brassica napus*) plants using a cotyledon-based strategy initially described by Moloney et al. (1989) and modified as described on the Biotechnology Resources for Arable Crop Transformation website (http://www.bract.org/transformationprotocols/transformationprotocols.html). All transgenic plants were generated in cv Pactol, except for the B_2 line, which was produced in cv Golda. *PPR-A* transgenic plants were multiplied by cross-pollination with fertile Pactol plants. Initial *PPR-B* transformants were selfed, and one plant out of the progeny of each line that subsequently produced 100% male-fertile plants (and therefore is potentially homozygous for the transgenes) was identified and used for all of the studies presented.

The SamRfo restored line was obtained by recurrent crossings of a rapeseed line carrying the *Rfo* radish (*Raphanus sativus*) locus with cv Samouraï (obtained from R. Delourme, Institut National de la Recherche Agronomique).

Characterization of Rapeseed Transformants by DNA Gel Blot Analysis

Genomic DNA was extracted for DNA hybridization analysis as described previously (Dellaporta et al., 1983) using fresh leaf samples harvested in the greenhouse. Total DNA was digested with the chosen restriction enzymes according to the manufacturer's instructions (Fermentas). The digestion products were electrophoresed on 0.8% (w/v) agarose gels in TBE buffer and then transferred to nylon membranes (GeneScreen). Hybridization and washes were performed at 65°C in hybridization buffer (0.5 M Na_2HPO_4, pH 7.4, 1 mM EDTA, and 7% [w/v] SDS), washing buffer I (2× SSPE [1× SSPE is 0.115 M NaCl, 10 mM sodium phosphate, and 1 mM EDTA, pH 7.4], 0.1% SDS, and 0.2% tetrasodium pyrophosphate), and washing buffer II (0.2× SSPE, 0.1% [w/v] SDS, and 0.2% [w/v] tetrasodium pyrophosphate), as described previously (Ausubel et al., 1990). *PPR-B*, *PPR-A*, and pEC2 probes were synthesized with the following primer pairs (see Supplemental Table 1 online): PPRA:18937U19 and PPRA:20954L21 for *PPR-A*, PPRB11560U21 and PPRB11950L16 for *PPR-B*, and pEC2:1396U21 and pEC2:2030L26 for pEC2.

In Situ Hybridization

Tissue fixation, embedding, sectioning, and in situ hybridization were done as described by Nikovics et al. (2006). Sense and antisense probes spanning the entire *orf138* coding sequence were synthesized by in vitro transcription and labeled with digoxigenin-UTP. DNA fragments used to generate the probes were PCR-amplified using primers T7-138-AS and orf138-3 for the sense probe and primers T7-138-S and orf138-2 for the antisense probe (see Supplemental Table 1 online). In order to prevent cross-hybridization with the high copy number of mitochondrial genomes likely present in metabolically active tissues, flower bud sections were first subjected to DNase I treatment (1.25 units/mL) for 20 min at 37°C before addition of proteinase K. Prehybridization, hybridization, and washing steps were performed at 42°C.

RT-PCR Analysis of *PPR-C*

RNA extraction, cDNA synthesis, and subsequent PCR amplification were performed as described previously (Arnal et al., 2006). The region of *PPR-C* mRNA spanning the hypothetical intron that would correct a frameshift mutation generated by a 17-bp deletion (Desloire et al., 2003) was PCR-amplified using primers PPRC2578U16 and PPRC3440L21 (see Supplemental Table 1 online). The PCR amplification product was visualized on an agarose gel with ethidium bromide, purified, and sequenced using PPRC2578U16 (see Supplemental Table 1 online), proving the absence of any intron sequence.

Protein Analysis

Production of Specific Polyclonal Antibodies against the PPR-B Protein

The *PPR-B* cDNA, except for the region encoding the mitochondrial targeting sequence, was amplified by PCR using the PPRBGW3 and PPRBGW5 primers (see Supplemental Table 1 online), and total cDNA was prepared from restored D81 radish buds. The BP recombination sequences were then completed in a second round of amplification with the oligonucleotides GW5 and GW3 (see Supplemental Table 1 online) and the first PCR mixture diluted 1:500. The amplified fragment obtained was then recombined into pDONR207 (Invitrogen) by the Gateway BP reaction, according to the manufacturer's recommendations. The *PPR-B* cDNA was subsequently incorporated by the Gateway LR reaction into the pDEST17 destination vector, creating a translational fusion of the PPR-B protein with six His residues. The fusion protein was expressed in strain BL21 (DE3) pLysS of *Escherichia coli*, solubilized with 8 M urea, and purified by metal-chelate column chromatography. The purified recombinant protein was then injected into rabbits for the production of polyclonal antiserum.

Rabbit anti-PPR-B IgGs were affinity-purified using purified recombinant PPR-B protein spotted onto a polyvinylidene fluoride membrane. The bound antibodies were eluted with five washes of 1 min each in 1 mL of a solution containing 50 mM Gly-HCl (pH 3), 500 mM NaCl, 0.25% (v/v) Tween 20, and 0.5% (w/v) BSA. After neutralization with 100 μL of 100 mM Tris-HCl (pH 7.8), the eluted antibodies were concentrated by ultrafiltration with a Vivaspin concentrator (Vivascience). Purified anti-PPR-B antibodies were used at a 1:1000 dilution in TBST for immunodetection experiments.

Preparation of Mitochondria

Mitochondria were isolated from floral buds with a maximum size of 4 mm following a modified protocol established for purification of *Arabidopsis thaliana* and tobacco (*Nicotiana benthamiana*) mitochondria (Millar et al., 2001). Flower buds were ground with a mortar and pestle and glass beads in grinding medium (300 mM sucrose, 25 mM tetrasodium pyrophosphate, 10 mM KH_2PO_4, 2 mM EDTA, 0.8% [w/v] polyvinylpyrrolidone-40, 0.3% [w/v] BSA, and 20 mM ascorbate, pH 7.5). Cell debris were removed by filtering the homogenate through a Miracloth membrane (Calbiochem). After three successive low-speed centrifugations at 2000, 2600, and 3000*g* for 10 min at 4°C, the supernatant was recovered and centrifuged at 23,400*g* for 20 min to pellet mitochondria. After resuspension in washing buffer (0.3 M sucrose and 10 mM HEPES-KOH, pH 7.5), organelles were loaded on Percoll density step gradients of 4, 5, and 3.5 mL containing, respectively, 50, 25, and 14% (v/v) of Percoll diluted in washing buffer supplemented with 0.2% BSA. After 20 min of centrifugation at 24,000*g* and 4°C, mitochondria were collected from the 50/25% interface, diluted at least 10 times in washing buffer, and pelleted at 23,400*g* for 20 min.

Preparation of Chloroplasts

Chloroplasts were isolated from 20 g of young leaves ground with a mortar and pestle in 50 mL of grinding medium (0.45 M sorbitol and 50 mM HEPES, pH 7.8). Following filtration through a Miracloth membrane (Calbiochem), the homogenate was spun for 3 min at 3000*g*. After resuspension in 4 mL of washing buffer (0.33 M sorbitol, 50 mM HEPES, pH 7.8, and 2.5 mM $MgCl_2$), crude chloroplast extracts were loaded onto

Percoll density step gradients of 1.5, 7, and 2.5 mL containing, respectively, 60, 35, and 20% (v/v) of Percoll diluted in washing buffer. After 15 min of centrifugation at 17,200*g* and 4°C, chloroplasts were collected from the 60/30% interface, diluted at least 10 times in washing buffer, and pelleted at 3000*g* for 2 min at 4°C.

Protein Immunodetection

Total proteins were extracted from various tissues and organelles, including flower buds of different sizes, anthers, flower buds from which anthers were removed, mitochondria isolated from flower buds, and chloroplasts purified from leaves. Protein concentrations were determined with the Bradford protein assay (Bio-Rad). Proteins were fractionated by SDS-PAGE, electrotransferred to polyvinylidene fluoride transfer membrane (Perkin-Elmer), and hybridized with polyclonal antibodies recognizing either PPR-B or ORF138, the ATPC protein (diluted 1:5000; a gift of Jörg Meurer, Ludwig-Maximilians-Universität), or with monoclonal antibodies recognizing the PORIN protein (diluted 1:500; a gift of David Day, University of Western Australia), or with various variants of the ribosomal protein RPL12 (diluted 1:2000; Delage et al., 2007). Binding of the primary antibodies was revealed by chemiluminescence using peroxidase-conjugated secondary antibodies (anti-rabbit IgG for the PPR-B and ORF138 antibodies and anti-mouse IgG for the PORIN antibodies) and enhanced chemiluminescence reagents (Amersham Pharmacia Biotech). The apparent molecular masses of the proteins were estimated with prestained molecular mass markers (Fermentas). At least two replicate experiments were performed for each analysis.

Analysis of the Submitochondrial Distribution of PPR-B

Soluble and membrane-bound mitochondrial proteins were prepared by lysing mitochondria with 1 mL of hypotonic buffer (20 mM HEPES, pH 7.7, 2 mM EDTA, and 1× Complete Protease Inhibitor Cocktail [Roche]) and forcing the mixture ~10 times through a 0.45- × 12-mm gauge needle. Unbroken mitochondria were pelleted by centrifugation for 10 min at 13,000*g*, and the supernatant was then centrifuged for 20 min at 100,000*g*. Soluble proteins contained in the supernatant were precipitated with trichloroacetic acid/acetone (50% trichloroacetic acid and 0.05% Triton X-100) and resuspended in loading buffer. The mitochondrial membranes contained in the pellet were briefly washed with 1 mL of hypotonic buffer, and proteins were directly extracted with 50 μL of 2× protein loading buffer. Peripheral (extrinsic) membrane proteins were extracted and solubilized from mitochondrial membranes by alkaline treatment (0.1 M sodium carbonate, pH 11.5) for 30 min at 4°C (Fujiki et al., 1982). Following treatment, mitochondrial membranes containing integral (intrinsic) membrane proteins and a fraction of incompletely removed extrinsic proteins were directly solubilized in 50 μL of 2× protein loading buffer. In addition to using the antibodies described above, the composition of each protein preparation was assessed using anti-NAD9 (Lamattina et al., 1993) and anti-formate dehydrogenase (des Francs-Small et al., 1992) antibodies.

Immunofluorescence Microscopy

Floral buds were fixed, embedded in low-melting-point wax (Aldrich), and processed for immunofluorescence as described by Baluska et al. (2002). Then, 8-μm sections were pretreated with 3% (w/v) BSA and incubated for 2 h with anti-ORF138 antiserum diluted 1:1000 (v/v) in PBS containing 0.1% (w/v) BSA. After rinsing in PBS, sections were incubated for 1 h with the anti-mouse secondary antibody Alexa Fluor 488 produced in goat (A-11017; Molecular Probes) diluted 1:500 in PBS supplemented with 0.1% (w/v) BSA. After additional rinses in PBS, sections were mounted under cover slips and examined using a Leica SP2 AOBS confocal laser-scanning microscope.

Protein/RNA Coimmunoprecipitation

Immunoprecipitation was performed essentially as described by Keene et al. (2006). Briefly, mitochondria were lysed in lysis buffer (10 mM HEPES-KOH, pH 7.7, 100 mM KCl, 5 mM $MgCl_2$, 0.5% [v/v] Triton X-100, and 2 mM DTT) supplemented with protease inhibitor cocktail (Roche), 0.2 mg/mL heparin, and 40 units of RNAsin (Fermentas). The lysis was performed by forcing the mix through a 0.45- × 12-mm gauge needle. After 30 min on ice, the extract was centrifuged for 10 min at 13,000*g* to pellet insoluble material and unbroken mitochondria. Twenty-five microliters of rProtein A Sepharose Fast Flow (Amersham Biosciences) suspension beads was briefly swollen in coimmunoprecipitation buffer (50 mM Tris-HCl, pH 7.5, 150 mM NaCl, 5 mM $MgCl_2$, 1 mM EDTA, 0.05% [w/v] Nonidet P-40, Roche protease inhibitor cocktail [used according to the manufacturer's instructions], and 0.2 mg/mL heparin) supplemented with 5% (w/v) BSA and 0.1 mg/mL yeast tRNA, then washed three times with coimmunoprecipitation buffer. Mitochondrial protein extracts were first precleared with the prepared rProtein A Sepharose beads for 10 min at 4°C, then centrifuged for 5 min at 11,000*g* to remove the beads from the extracts. Ten microliters of purified PPR-B antibody (or 1 μL of anti-formate dehydrogenase antibody as a control) was added to ~3 mg of mitochondrial proteins and incubated for 3 h at 4°C with gentle rotation. The protein extract was transferred onto a second batch of rProtein A Sepharose beads equilibrated in coimmunoprecipitation buffer and further incubated for 60 min at 4°C with gentle rotation. Supernatants were collected by low-speed centrifugation, and the beads were washed three times with 250 μL of coimmunoprecipitation buffer. RNA was recovered from the pellet and the supernatant by phenol extraction as described by Ostheimer et al. (2003). Half of the RNA from coimmunoprecipitation pellets and one-fifteenth from the supernatants were applied to a nylon membrane (GeneScreen hybridization transfer membrane; NENTM Life Science Products) with a slot-blot manifold (Schleicher and Schuell) and hybridized with radiolabeled probes specific to the *orf138* and *cox2* mRNAs. PCR fragments amplified with orf138-1 and orf138-2 primers and with Bncox2-3 and Bncox2-5 primers (see Supplemental Table 1 online) were radiolabeled with [α-^{32}P]dCTP by random priming (Prime-a-Gene labeling system; Promega) and then purified on Micro Bio-Spin P-30 Tris chromatography columns (Bio-Rad). Slot-blot membranes were hybridized overnight in 7% (w/v) SDS and 0.5 M tetrasodium phosphate, pH 7, at 65°C. Blots were washed in 2× SSC, 0.1% (w/v) SDS and in 1× SSC, 0.1% (w/v) SDS for 15 min each and then in 0.1× SSC, 0.1% (w/v) SDS at 65°C for 30 min. Hybridization signals were revealed by autoradiography or by exposure to phosphor imaging plates (Fuji), which were subsequently scanned with a BAS5000 phosphor imager (Fuji).

Accession Numbers

Sequence data from this article can be found in the GenBank/EMBL data libraries under accession numbers FJ455099 (*PPR-B-LIKE1*) and AJ550021 (*Rfo* locus).

Supplemental Data

The following materials are available in the online version of this article.

Supplemental Figure 1. Analysis of the Efficacy of an Antiserum in Recognizing PPR-B and PPR-B–Related Proteins in Mitochondrial Protein Extracts.

Supplemental Figure 2. The Anti-PPR-B Antiserum Detects the PPR-A and PPR-B Proteins with Similar Sensitivities.

Supplemental Figure 3. A PPR-B Presequence–Green Fluorescent Protein Fusion Is Targeted to Tobacco Mitochondria.

Supplemental Table 1. Primers Used in This Study.

ACKNOWLEDGMENTS

We thank Olivier Grandjean for technical assistance with the confocal microscopy, Halima Morin for her help with the in situ hybridization experiments, and Catherine Primard-Brisset and Catherine Jeudy for helping to produce the transgenic plants. We are also grateful to Jörg Meurer for providing antiserum raised against ATPC. M.U. was supported by a Ph.D. fellowship from the Institut National de la Recherche Agronomique.

Received November 28, 2007; revised October 31, 2008; accepted December 5, 2008; published December 19, 2008.

REFERENCES

Arnal, N., Alban, C., Quadrado, M., Grandjean, O., and Mireau, H. (2006). The Arabidopsis Bio2 protein requires mitochondrial targeting for activity. Plant Mol. Biol. **62:** 471–479.

Ausubel, F.M., Brent, R., Kingston, R.E., Moore, D.D., Seidman, J.G., Smith, J.A., and Struhl, K. (1990). Current Protocols in Molecular Biology. (New York: John Wiley & Sons).

Baluska, F., Hlavacka, A., Samaj, J., Palme, K., Robinson, D.G., Matoh, T., McCurdy, D.W., Menzel, D., and Volkmann, D. (2002). F-actin-dependent endocytosis of cell wall pectins in meristematic root cells. Insights from brefeldin A-induced compartments. Plant Physiol. **130:** 422–431.

Bedinger, P. (1992). The remarkable biology of pollen. Plant Cell **4:** 879–887.

Beick, S., Schmitz-Linneweber, C., Williams-Carrier, R., Jensen, B., and Barkan, A. (2008). The pentatricopeptide repeat protein PPR5 stabilizes a specific tRNA precursor in maize chloroplasts. Mol. Cell. Biol. **28:** 5337–5347.

Bellaoui, M., Grelon, M., Pelletier, G., and Budar, F. (1999). The restorer Rfo gene acts post-translationally on the stability of the ORF138 Ogura CMS-associated protein in reproductive tissues of rapeseed cybrids. Plant Mol. Biol. **40:** 893–902.

Bentolila, S., Alfonso, A.A., and Hanson, M.R. (2002). A pentatricopeptide repeat-containing gene restores fertility to cytoplasmic male-sterile plants. Proc. Natl. Acad. Sci. USA **99:** 10887–10892.

Bonhomme, S., Budar, F., Férault, M., and Pelletier, G. (1991). A 2.5 kb *Nco*I fragment of Ogura radish mitochondrial DNA is correlated with cytoplasmic male-sterility in *Brassica* cybrids. Curr. Genet. **19:** 121–127.

Bonhomme, S., Budar, F., Lancelin, D., Small, I., Defrance, M.C., and Pelletier, G. (1992). Sequence and transcript analysis of the Nco2.5 Ogura-specific fragment correlated with cytoplasmic male sterility in Brassica cybrids. Mol. Gen. Genet. **235:** 340–348.

Brown, G.G., Formanova, N., Jin, H., Wargachuk, R., Dendy, C., Patil, P., Laforest, M., Zhang, J., Cheung, W.Y., and Landry, B.S. (2003). The radish Rfo restorer gene of Ogura cytoplasmic male sterility encodes a protein with multiple pentatricopeptide repeats. Plant J. **35:** 262–272.

Cartea, M.E., Migdal, M., Galle, A.M., Pelletier, G., and Guerche, P. (1998). Comparison of sense and antisense methodologies for modifying the fatty acid composition of *Arabidopsis thaliana* oilseed. Plant Sci. **136:** 181–194.

Chase, C.D. (2007). Cytoplasmic male sterility: A window to the world of plant mitochondrial-nuclear interactions. Trends Genet. **23:** 81–90.

Delage, L., Giegé, P., Sakamoto, M., and Maréchal-Drouard, L. (2007). Four paralogues of RPL12 are differentially associated to ribosome in plant mitochondria. Biochimie **89:** 658–668.

Dellaporta, J., Wood, J., and Hicks, J. (1983). A plant DNA minipreparation: Version II. Plant Mol. Biol. Rep. **1:** 19–21.

de Longevialle, A.F., Hendrickson, L., Taylor, N.L., Delannoy, E., Lurin, C., Badger, M., Millar, A.H., and Small, I. (2008). The pentatricopeptide repeat gene OTP51 with two LAGLIDADG motifs is required for the cis-splicing of plastid ycf3 intron 2 in *Arabidopsis thaliana*. Plant J. **56:** 157–168.

de Longevialle, A.F., Meyer, E.H., Andrés, C., Taylor, N.L., Lurin, C., Millar, A.H., and Small, I.D. (2007). The pentatricopeptide repeat gene OTP43 is required for trans-splicing of the mitochondrial NAD1 intron 1 in *Arabidopsis thaliana*. Plant Cell **19:** 3256–3265.

Delourme, R., Foisset, N., Horvais, R., Barret, P., Champagne, G., Cheung, W.Y., Landry, B.S., and Renard, M. (1998). Characterisation of the radish introgression carrying the Rfo restorer gene for the Ogu-INRA cytoplasmic male sterility in rapeseed (*Brassica napus* L.). Theor. Appl. Genet. **97:** 129–134.

des Francs-Small, C.C., Ambard-Bretteville, F., Darpas, A., Sallantin, M., Huet, J.-C., Pernollet, J.-C., and Rémy, R. (1992). Variation of the polypeptide composition of mitochondria isolated from different potato tissues. Plant Physiol. **98:** 273–278.

Desloire, S., et al. (2003). Identification of the fertility restoration locus, Rfo, in radish, as a member of the pentatricopeptide-repeat protein family. EMBO Rep. **4:** 588–594.

Duroc, Y., Gaillard, C., Hiard, S., Defrance, M.C., Pelletier, G., and Budar, F. (2005). Biochemical and functional characterization of ORF138, a mitochondrial protein responsible for Ogura cytoplasmic male sterility in Brassicaceae. Biochimie **87:** 1089–1100.

Fisk, D.G., Walker, M.B., and Barkan, A. (1999). Molecular cloning of the maize gene CRP1 reveals similarity between regulators of mitochondrial and chloroplast gene expression. EMBO J. **18:** 2621–2630.

Fox, T.D. (1996). Genetics of mitochondrial translation. In Translational Control, J.W.B. Hershey, M.B. Matthews, N. Sonenberg, eds (Cold Spring Harbor, NY: Cold Spring Harbor Laboratory Press), pp. 733–758.

Fujiki, Y., Hubbard, A.L., Fowler, S., and Lazarow, P.B. (1982). Isolation of intracellular membranes by means of sodium carbonate treatment: Application to endoplasmic reticulum. J. Cell Biol. **93:** 97–102.

Geddy, R., and Brown, G.G. (2007). Genes encoding pentatricopeptide repeat (PPR) proteins are not conserved in location in plant genomes and may be subject to diversifying selection. BMC Genomics **8:** 130.

Giancola, S., Marhadour, S., Desloire, S., Clouet, V., Falentin-Guyomarc'h, H., Laloui, W., Falentin, C., Pelletier, G., Renard, M., Bendahmane, A., Delourme, R., and Budar, F. (2003). Characterization of a radish introgression carrying the Ogura fertility restorer gene Rfo in rapeseed, using the Arabidopsis genome sequence and radish genetic mapping. Theor. Appl. Genet. **107:** 1442–1451.

Gillman, J.D., Bentolila, S., and Hanson, M.R. (2007). The petunia restorer of fertility protein is part of a large mitochondrial complex that interacts with transcripts of the CMS-associated locus. Plant J. **49:** 217–227.

González-Melendi, P., Uyttewaal, M., Morcillo, C.N., Hernández Mora, J.R., Fajardo, S., Budar, F., and Lucas, M.M. (2008). A light and electron microscopy analysis of the events leading to male sterility in Ogu-INRA CMS of rapeseed (*Brassica napus*). J. Exp. Bot. **59:** 827–838.

Gourret, J.P., Delourme, R., and Renard, M. (1992). Expression of *ogu* cytoplasmic male sterility in cybrids of *Brassica napus*. Theor. Appl. Genet. **83:** 549–556.

Grelon, M., Budar, F., Bonhomme, S., and Pelletier, G. (1994). Ogura cytoplasmic male-sterility (CMS)-associated orf138 is translated into a mitochondrial membrane polypeptide in male-sterile Brassica cybrids. Mol. Gen. Genet. **243:** 540–547.

Hanson, M.R., and Bentolila, S. (2004). Interactions of mitochondrial and nuclear genes that affect male gametophyte development. Plant Cell **16** (suppl.): S154–S169.

Hashimoto, M., Endo, T., Peltier, G., Tasaka, M., and Shikanai, T. (2003). A nucleus-encoded factor, CRR2, is essential for the expression of chloroplast ndhB in Arabidopsis. Plant J. **36:** 541–549.

Hattori, M., Miyake, H., and Sugita, M. (2007). A pentatricopeptide repeat protein is required for RNA processing of clpP pre-mRNA in moss chloroplasts. J. Biol. Chem. **282:** 10773–10782.

Kazama, T., Nakamura, T., Watanabe, M., Sugita, M., and Toriyama, K. (2008). Suppression mechanism of mitochondrial ORF79 accumulation by Rf1 protein in BT-type cytoplasmic male sterile rice. Plant J. **55:** 619–628.

Keene, J.D., Komisarow, J.M., and Friedersdorf, M.B. (2006). RIP-Chip: The isolation and identification of mRNAs, microRNAs and protein components of ribonucleoprotein complexes from cell extracts. Nat. Protocols **1:** 302–307.

Klein, R.R., Klein, P.E., Mullet, J.E., Minx, P., Rooney, W.L., and Schertz, K.F. (2005). Fertility restorer locus Rf1 of sorghum (*Sorghum bicolor* L.) encodes a pentatricopeptide repeat protein not present in the colinear region of rice chromosome 12. Theor. Appl. Genet. **111:** 994–1012.

Koizuka, N., Imai, R., Fujimoto, H., Hayakawa, T., Kimura, Y., Kohno-Murase, J., Sakai, T., Kawasaki, S., and Imamura, J. (2003). Genetic characterization of a pentatricopeptide repeat protein gene, orf687, that restores fertility in the cytoplasmic male-sterile Kosena radish. Plant J. **34:** 407–415.

Kotera, E., Tasaka, M., and Shikanai, T. (2005). A pentatricopeptide repeat protein is essential for RNA editing in chloroplasts. Nature **433:** 326–330.

Krause, K., Lopes de Souza, R., Roberts, D.G.W., and Dieckmann, C.L. (2004). The mitochondrial message-specific mRNA protectors Cbp1 and Pet309 are associated in a high-molecular weight complex. Mol. Biol. Cell **15:** 2674–2683.

Krishnasamy, S., and Makaroff, C.A. (1994). Organ-specific reduction in the abundance of a mitochondrial protein accompanies fertility restoration in cytoplasmic male-sterile radish. Plant Mol. Biol. **26:** 935–946.

Lahmy, S., Barneche, F., Derancourt, J., Filipowicz, W., Delseny, M., and Echeverria, M. (2000). A chloroplastic RNA-binding protein is a new member of the PPR family. FEBS Lett. **480:** 255–260.

Lamattina, L., Gonzalez, D., Gualberto, J., and Grienenberger, J.M. (1993). Higher plant mitochondria encode an homologue of the nuclear-encoded 30-kDa subunit of bovine mitochondrial complex I. Eur. J. Biochem. **217:** 831–838.

Lurin, C., et al. (2004). Genome-wide analysis of Arabidopsis pentatricopeptide repeat proteins reveals their essential role in organelle biogenesis. Plant Cell **16:** 2089–2103.

Meierhoff, K., Felder, S., Nakamura, T., Bechtold, N., and Schuster, G. (2003). HCF152, an Arabidopsis RNA binding pentatricopeptide repeat protein involved in the processing of chloroplast psbB-psbT-psbH-petB-petD RNAs. Plant Cell **15:** 1480–1495.

Millar, A.H., Liddel, A., and Leaver, C.J. (2001). Isolation and subfractionation of mitochondria from plants. Methods Cell Biol. **1:** 53–74.

Moloney, M.M., Walker, J.M., and Sharma, K.K. (1989). High efficiency transformation of *Brassica napus* using *Agrobacterium* vectors. Plant Cell Rep. **8:** 238–242.

Nakamura, T., Meierhoff, K., Westhoff, P., and Schuster, G. (2003). RNA-binding properties of HCF152, an Arabidopsis PPR protein involved in the processing of chloroplast RNA. Eur. J. Biochem. **270:** 4070–4081.

Nikovics, K., Blein, T., Peaucelle, A., Ishida, T., Morin, H., Aida, M., and Laufs, P. (2006). The balance between the *MIR164A* and *CUC2* genes controls leaf margin serration in Arabidopsis. Plant Cell **18:** 2929–2945.

Okuda, K., Myouga, F., Motohashi, R., Shinozaki, K., and Shikanai, T. (2007). Conserved domain structure of pentatricopeptide repeat proteins involved in chloroplast RNA editing. Proc. Natl. Acad. Sci. USA **104:** 8178–8183.

Ostheimer, G.J., Williams-Carrier, R., Belcher, S., Osborne, E., Gierke, J., and Barkan, A. (2003). Group II intron splicing factors derived by diversification of an ancient RNA-binding domain. EMBO J. **22:** 3919–3929.

O'Toole, N., Hattori, M., Andres, C., Iida, K., Lurin, C., Schmitz-Linneweber, C., Sugita, M., and Small, I. (2008). On the expansion of the pentatricopeptide repeat gene family in plants. Mol. Biol. Evol. **25:** 1120–1128.

Richter, T.E., and Ronald, P.C. (2000). The evolution of disease resistance genes. Plant Mol. Biol. **42:** 195–204.

Schmitz-Linneweber, C., Williams-Carrier, R., and Barkan, A. (2005). RNA immunoprecipitation and microarray analysis show a chloroplast pentatricopeptide repeat protein to be associated with the 5′ region of mRNAs whose translation it activates. Plant Cell **17:** 2791–2804.

Schmitz-Linneweber, C., Williams-Carrier, R.E., Williams-Voelker, P.M., Kroeger, T.S., Vichas, A., and Barkan, A. (2006). A pentatricopeptide repeat protein facilitates the trans-splicing of the maize chloroplast rps12 pre-mRNA. Plant Cell **18:** 2650–2663.

Small, I.D., and Peeters, N. (2000). The PPR motif—A TPR-related motif prevalent in plant organellar proteins. Trends Biochem. Sci. **25:** 46–47.

Touzet, P., and Budar, F. (2004). Unveiling the molecular arms race between two conflicting genomes in cytoplasmic male sterility? Trends Plant Sci. **9:** 568–570.

Uyttewaal, M., Mireau, H., Rurek, M., Hammani, K., Arnal, N., Quadrado, M., and Giegé, P. (2008). PPR336 is associated with polysomes in plant mitochondria. J. Mol. Biol. **375:** 626–636.

Wang, Z., et al. (2006). Cytoplasmic male sterility of rice with boro II cytoplasm is caused by a cytotoxic peptide and is restored by two related PPR motif genes via distinct modes of mRNA silencing. Plant Cell **18:** 676–687.

Williams-Carrier, R., Kroeger, T., and Barkan, A. (2008). Sequence-specific binding of a chloroplast pentatricopeptide repeat protein to its native group II intron ligand. RNA **14:** 1930–1941.

Yamazaki, H., Tasaka, M., and Shikanai, T. (2004). PPR motifs of the nucleus-encoded factor, PGR3, function in the selective and distinct steps of chloroplast gene expression in Arabidopsis. Plant J. **38:** 152–163.